Dalton Transactions

Accepted Manuscript

ROYAL SOCIETY OF CHEMISTRY

www.rsc.org/dalton

Journal Name

RSCPublishing

ARTICLE

Cite this: DOI: 10.1039/x0xx00000x

Received 00th January 2012,
Accepted 00th January 2012

DOI: 10.1039/x0xx00000x

www.rsc.org/

The specificity of interaction of Zn^{2+}, Ni^{2+} and Cu^{2+} ions with the histidine-rich domain of TjZNT1 ZIP family transporter

Slawomir Potocki,[a] Daniela Valensin[b] and Henryk Kozlowski[a]

The Zrt/Irt-like protein (ZIP) family contributes to the metal homeostasis by regulating transport of divalent metal cations such as Fe^{2+}, Zn^{2+}, Mn^{2+}, Cd^{2+} sometimes even Cu^{2+}. Most ZIP members have a long variable loop between transmembrane domains (TMDs) III and IV; this region is predicted to be located in the cytoplasm and is postulated to be the metal ion binding site. In this study, we looked on the thermodynamic behavior and coordination chemistry of Zn^{2+}, Ni^{2+} and Cu^{2+} complexes with the histidine-rich domain, Ac-(185)RAHAAHHRHSH(195)-NH_2 (HRD), from yeast TjZNT1 protein, located between TMD III and IV. The sequence is conserved also in higher species like *Thlaspi japonicum*. The stability of complexes increase in the series $Ni^{2+} < Zn^{2+} << Cu^{2+}$. The geometry of complexes is very different for each metal and in the case of Zn^{2+} complexes, high specificity in binding is observed. Moreover, stability of HRD-Cu^{2+} complexes was compared with the five His residues containing peptide from Hpn protein (*Helicobacter pylori*). The results suggest high ability of HRD in the binding of all three studied metals.

Introduction

The ZIP proteins belong to the important family of transporters that deliver divalent metal ions from extracellular space into the cytoplasm.[1-4] They has been extensively studied in recent years. The reason for this is not only, that not much is known about their mechanism of action, but also because of their similarity to prion proteins in the sense of structure, distribution and possible functions in the living organisms.[5,6] ZIPs have some specific, interesting, often unstructured regions, which have been investigated more intensively.[7-9] The example is N-terminus, which seems to be very much like the one present in prion proteins, especially in ZIP 5, 6 and 10.[5] Its coordination abilities of various metals e.g. Bi^{3+}, Ni^{2+}, Zn^{2+} and Cd^{2+} is very high because of the presence of Cys residues.[7] Moreover, studies on a series of TjZNT1 and TjZNT2 chimeric genes of *Thlaspi japonicum* revealed metal selectivity of N-terminus. As a result, the extracellular N-terminal ends are identified as a regions involved in metal ions selectivity; N-terminal region appeared to be a novel substrate selector (e.g. for Zn^{2+} and Mn^{2+}) in the ZIP family proteins.[10]

As far as functional regions involved in metal ions selectivity are concerned, the loop between the transmembrane domain II and III should be considered. It has been shown, that the replacement of a Glu residue at position 103 in wild-type IRT1 protein (ZIP family) with Ala, changes the substrate specificity of the transporter by selectively eliminating its ability to transport Zn^{2+}.[8] Other mutations, increase or reduce IRT1 selectivity binding towards different metal ions. A number of other conserved residues in or near TMDs appear to be essential for all transporting functions. Some of the residues important for substrate selection and transport in a protein belonging to the ZIP gene family have been identified. The chemical studies on the IRT1 loop, Ac-(95)MHVLPDSFEMLSSICLEENPWHK(117)-NH_2, have shown high impact of Glu residues in the formation of Zn^{2+} complexes.[9]

The proteins from ZIP families of Zn^{2+} transporters, contain a histidine-rich sequence in a loop domain located between TMDs III and IV. Topological investigations suggest that these loops are located in the cytoplasm and contain a His-rich domains (HRDs). Those HRDs were postulated to serve as metal binding site in ZIP family proteins.[11] Directed-mutagenesis studies on hZip1 human zinc transporter suggest that both histidines from the sequence (158)HWHD(161) are necessary for the Zn^{2+} transport, however substitution of His residues with Ala do not affect plasma membrane localization of the transporter.[11] Similar observations were reported for the Zrt1 transporter in yeast.[12] However, HRDs role has not been fully determined yet and the contradictory thesis on their involvement in metal ions transport are proposed. Deletion of the HRD does not affect the Ni^{2+} tolerance ability of TjZNT, ZIP family transporter that confers high Ni^{2+} tolerance to yeast.[13] Moreover, the deletion of HRD increases the proteins specificity for Zn^{2+} but not for Cd^{2+}. Simultaneously, subcellular localizations of TjZNT1 (green fluorescent protein studies) are not affected.[14] On the other hand, mutations in the HRD of human ZIP1 and ZIP4 results in a reduction in cellular Zn^{2+} uptake.[11,15] Other results suggest that HRDs are essential for Zn-stimulated ubiquitination and degradation of the protein.[15] As it has been recently shown, the HRD in the one of the Cation Diffusion Facilitator (CDF) protein, also transmembrane transporter, binds metal ions and is considered to be involved in metal recognition.[16,17] What is more clear about ZIP proteins, the expression is controlled by metals concentration and protein accumulation.[18] However, the role of particular domains remain unclear.

Studies on TjZNT1 and TjZNT2 genes from the Ni^{2+} hyperaccumulator *Thlaspi japonicum* found these transporters to be in charge of high Ni^{2+} tolerance in yeast.[19] On the other hand, the participation of the HRD of TjZNT1 in the ability of this protein to affect Ni^{2+} tolerance is neglected, since the deletion of the HRD did not affect Ni^{2+} tolerance level.[20] Unlike many ZIP members that have one HRD, TjZNT1 and TjZNT2 have two long HRDs between III and IV TMD. It is well known that histidine can effectively bind Zn^{2+}, Ni^{2+} and Cu^{2+} ions[21-23] free histidine residues are also involved in Ni^{2+} loading and detoxification in plants.[24] Investigations on the effect of HRD deletion on the transport ability of TjZNT1 proved that the HRD affects the specificity for Zn^{2+}.[14] In this study, we propose meticulous coordination chemistry studies on 11-aminoacid sequence Ac-(185)RAHAAHHRHSH(195)-NH_2 (HRD), domain from the loop between TMD III and IV from TjZNT1 protein of yeasts. The results suggest, that the Zn^{2+} complexes stability is higher than those of Ni^{2+}. Moreover, Zn^{2+} ions exhibit some kind of a binding specificity for such a short fragment of the protein. With comparison to Zn^{2+} and Ni^{2+} ions, Cu^{2+} reflects outstanding stability with the studied HRD fragment.

Results and discussion

HRD ligand

The HRD peptide studied here behaves as H_5L acid (Tab. 1). All five pK values, 7.21, 6.45, 6.14, 5.73, 5.05, were assigned to His imidazoles. The values are in good agreement with the literature data for comparable systems.[25,26]

Zn^{2+} complexes

Zinc binding to HRD was investigated by potentiometric, NMR and mass spectrometry techniques. The distribution diagram and all the calculated pK constants are shown in Fig. 1 and Tab 1. Four different Zn^{2+} species were detected: ZnHL is the first one, where three His residues are already bound. The second one, and simultaniously most abundant one, which dominates over 6.0–8.5 pH range is ZnL. The number of coordinated imidazoles does not change during the last His deprotonation. The ZnL logβ is 5.88, what is distinctly lower than the one obtained for [$3N_{im}$-N_{term}] coordination of a peptide with similar length and sequence from zebra fish prion-like protein[27] and similar to 3-His containing peptides[21] suggesting in this particular case the involvement of three imidazoles in the metal ion binding. Because Zn^{2+} tends to form tetrahedral geometry complexes, the fourth coordination sphere is accomplished by water molecule. At higher pH, hydroxo species are formed.

Tab. 1. Potentiometric data for proton, Zn^{2+}, Ni^{2+} and Cu^{2+} complexes of Ac-RAHAAHHRHSH-NH_2 peptide.

	log*β*	p*K*
HL	7.21(3)	7.21
H_2L	13.66(2)	6.45
H_3L	19.80(1)	6.14
H_4L	25.53(2)	5.73
H_5L	30.58(1)	5.05
ZnHL	12.44(2)	
ZnL	5.88(2)	6.56
$ZnH_{-1}L$	-1.71(0)	7.59
$ZnH_{-2}L$	-10.43(6)	8.72
NiHL	11.31(1)	
NiL	4.52(2)	6.78
$NiH_{-1}L$	-4.24(7)	8.77
$NiH_{-3}L$	-22.17(5)	
CuH_3L	28.06(1)	
CuHL	18.97(3)	
CuL	13.76(2)	5.21
$CuH_{-1}L$	6.50(1)	7.26
$CuH_{-2}L$	-1.27(2)	7.77
$CuH_{-3}L$	-10.67(1)	9.40

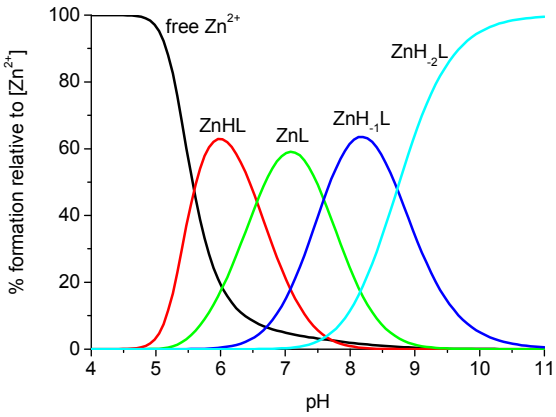

Fig. 1. Species distribution profiles for Zn^{2+} complexes of Ac-RAHAAHHRHSH-NH_2 peptide. Metal to ligand ratio = 1:1; [metal] = 1 x 10^{-3} M.

The full characterization of zinc complexes was obtained by analyzing ^{1}H-^{1}H TOCSY NMR spectra recorded for ligand itself and in the presence of different amounts of the metal ion at pH 7.00 (ZnL range). Addition of Zn^{2+} to HRD yielded strong variations on several proton signals. The diamagnetic nature of the metal allowed the addition of up to 0.9 equivalents of Zn^{2+} to HRD solution. The presence of Zn^{2+} caused both shifts and broadening of the NMR resonances. Three of five εH aromatic protons are strongly affected, particularly those from His-190, His-191 and His-193 (Fig. 2). The largest broadening was detected in the presence of 0.5 equivalents of Zn^{2+} (Fig. 2) suggesting the occurrence of comparable amounts of the apo and Zn^{2+} bound forms at this metal ratio. Unfortunately, no distinguishable changes on ^{1}H-^{1}H TOCSY resonances was observed in aliphatic region. All correlations of His βH (which also may confirm the process of complex formation) are overlapped and are not useful in the identification of His residues.

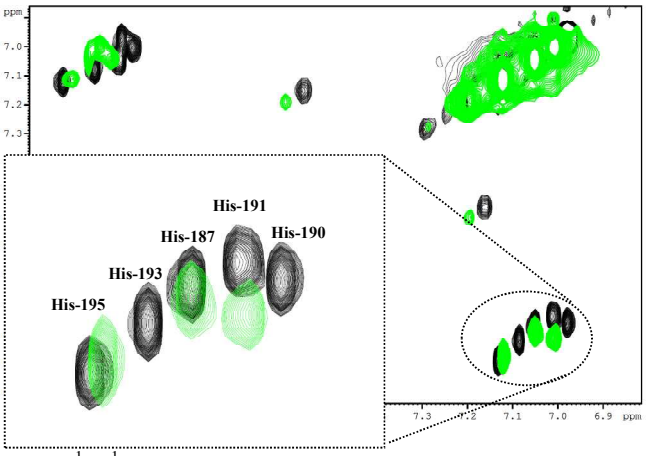

Fig. 2. ^{1}H-^{1}H TOCSY spectra of Ac-RAHAAHHRHSH-NH_2, 1 x 10^{-3} M, pH 7.0, T 300 K in absence (black) and in presence (green) of 0.75 Zn^{2+} eqs.

Mass spectrometry results confirmed 1:1 binding. Molecular mass of the HRD peptide is 1357.45 Da ($C_{56}H_{84}N_{28}O_{13}$). Upon the addition of Zn^{2+} ions to the peptide, only the formation of equimolar species can be observed. The highest intensity of the peptide itself and of its Na^+ and Zn^{2+} complexes was recorded for a +2 charged species, with the m/z ratio 710.30 for Zn^{2+} complex (Fig. 3).

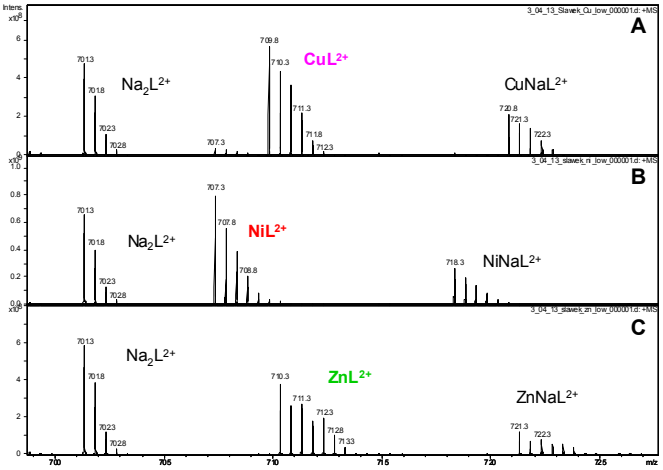

Fig. 3. ESI MS spectra of a system containing HRD with Cu^{2+} (A), Ni^{2+} (B), and Zn^{2+} (C) ions.

Ni^{2+} complexes

Methods used for Ni^{2+} complexes investigations have been enriched by UV-Vis and CD. Those techniques give more insight into geometry of formed in solution complexes. As far as the Ni^{2+}-HRD complexes are concerned, MS data clearly shows, that all species are equimolar complexes (Fig. 3). Potentiometric titrations together with spectroscopic measurements provided us with the information about the stability of the complex and about the nickel binding sites. During potentiometric calculations, four Ni^{2+} complex species were identified (Fig. 4). The first species of Ni^{2+} NiHL, reaches maximum concentration at pH ≈6 (Table 1, Fig. 4). This is most probably a paramagnetic multi-imidazole complex. The next deprotonation lead to the formation of NiL species, due to the dissociation of the consecutive imidazole proton. No distinct charge transfer N → Ni^{2+}, neither strong d–d transitions could be observed in the CD and UV-Vis spectra below pH 8.3 (Fig. 5), which excludes the coordination of amide nitrogens. The spectroscopic data of the $NiH_{-1}L$ and $NiH_{-3}L$ species could be properly assigned. The formation of $NiH_{-1}L$ complex starts at pH 7.0 and it dominates at pH 9.0. Charge transfer band typical for N_{im} → Ni^{2+} (260 - 270 nm) and N^- → Ni^{2+} (250 – 270 nm)[28] is observed (Fig. 5). The spectroscopic parameters are consistent with a 4 N {$1N^-$,$3N_{im}$} donor set; in particular the UV–Vis maximum at 430 nm with ε = 125 (M^{-1} cm^{-1}) and CD spectra with a distinct d-d bands at 425 nm and 550 nm show that the $NiH_{-1}L$ species has already a squareplanar geometry.[29,30] Above pH 9.5 the UV-Vis band with maximum at 430 nm is still rising suggesting the participation of another N^- amide nitrogens in the metal ion binding.

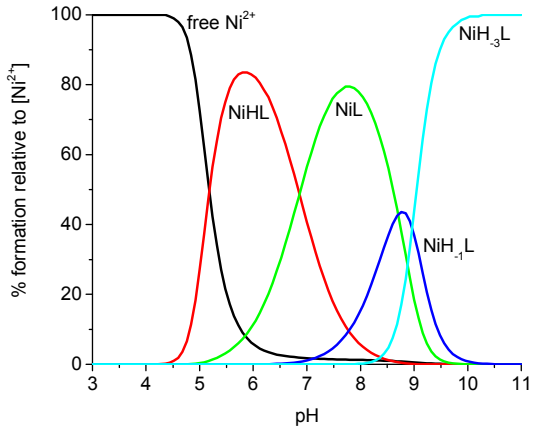

Fig. 4. Species distribution profiles for Ni^{2+} complexes of Ac-RAHAAHHRHSH-NH_2 peptide. Metal to ligand ratio = 1:1; [metal] = 1 x 10^{-3} M.

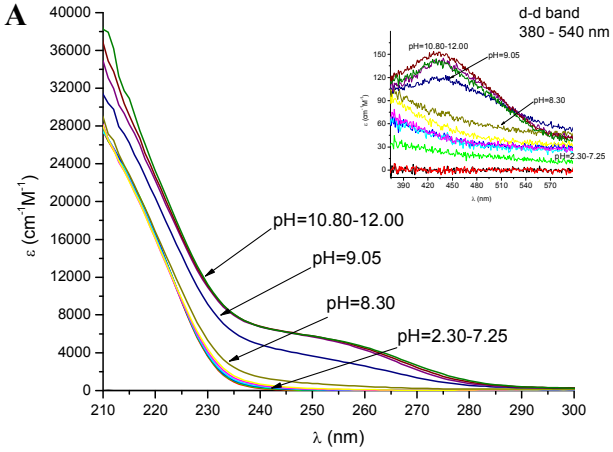

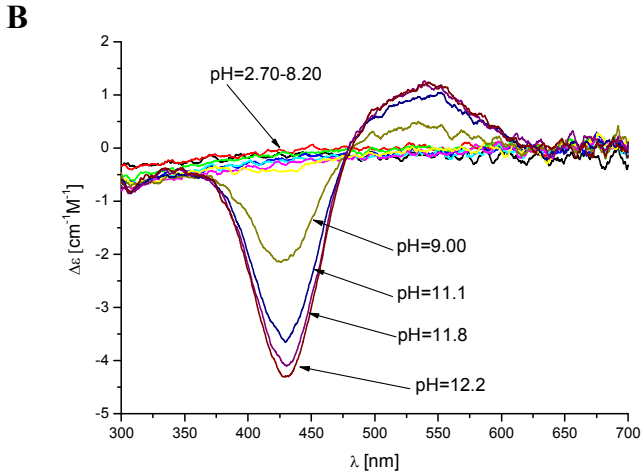

Fig. 5. UV-Vis (A) and CD spectra (B) for Ni^{2+} complex of Ac-RAHAAHHRHSH-NH_2 peptide. Metal to ligand ratio = 1:1; [metal] = 1 x 10^{-3} M.

The $NiH_{-3}L$ HRD species was further characterized by using NMR spectroscopy. We found that proton spin-lattice relaxation rates (R_1) measured for the Ni^{2+} complex at pH 10 were similar to those of the free ligand, strongly suggesting the formation of diamagnetic metal bound species, which explains the strong shifts observed for ^1H (Fig. 6.). The formation of diamagnetic complex allowed us to detect the metal binding sites. After the addition of 0.9 Ni^{2+} eqs. of ions addition, selective chemical shift variations were detected by comparing ^1H-^1H 2D TOCSY experiments recorded for apo and Ni^{2+} bound forms (Fig. 6). The water solubility of the ligand was high enough to obtain fully reliable NMR spectra, much information regarding the behavior of the ligand towards Ni^{2+} ions has been obtained. Until pH 8, paramagnetic species are mainly present; diamagnetic species start to appear in the NMR spectra at higher pH, what is in agreement with the potentiometric, UV-Vis and CD results. Unfortunately, even slow titration with a Ni^{2+} ions did not answer the question which His residues are preferable in binding. Looking at the shift of Ser-194 and Arg-192 (Fig. 6) we may conclude, that C-terminus of a peptide is somewhat preferable, but on the other hand chemical shifts of Ala residues are observed since the very beginning of HRD titration with Ni^{2+}, strongly suggesting more than one possible mode of binding.

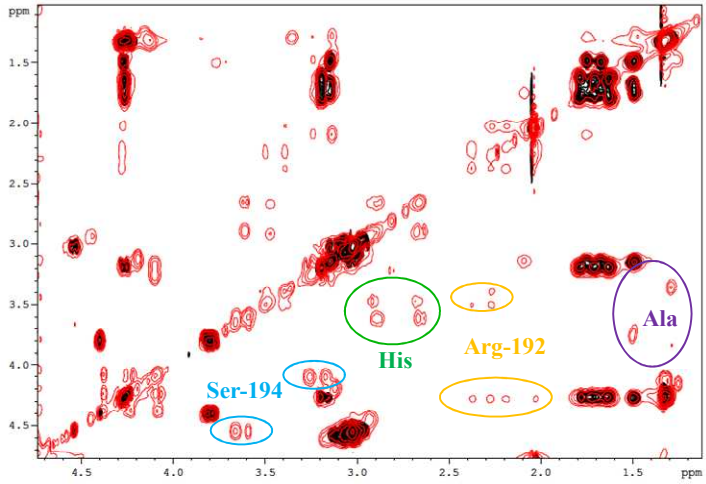

Fig. 6. ^1H-^1H TOCSY spectra of Ac-RAHAAHHRHSH-NH_2,1 x 10^{-3} M, pH 10.0, T 300 K in absence (black) and in presence (red) of 0.75 Ni^{2+} eqs.

Cu^{2+} complexes

For unstructured peptides, the best binding sites for Cu^{2+} are N-donors, derived from imidazole of His, amino groups of N-terminal and backbone amide nitrogens.[34,35] Mass spectrometry results show 1:1 binding stoichiometry (Fig. 3). The calculations based on the pH titrations of HRD–Cu^{2+} complexes in 4mM HCl (0.1M KCl) suggest the formation of six mononuclear species (Fig. 7). Since the number of species is relatively high and they are partly overlapped, the assignment of the spectroscopic data was possible only for the major complexes. In the first observed species, CuH_3L with a maximum at pH 4.0, two His residues are already deprotonated and bound to Cu^{2+} ion what arises straight forward from potentiometric diagram (decrease of free Cu^{2+} amount) and bands on UV-Vis spectra at 320 nm (charge transfer $N_{im} \rightarrow Cu^{2+}$) and d-d transition at 630 nm. The CuHL species is formed by loosing another two imidazole protons from His residues. A big jump in the intensity of the charge transfer and

d-d transition bands in UV-Vis spectrum, suggest the involvement of both deprotonated His residues in metal ion binding resulting in the $4N_{im}$ coordination mode. This complex species reaches the maximum at pH 5.0. The d–d band at 630 nm with ε = 60 $M^{-1}cm^{-1}$ (Fig. 8) and EPR parameters $A_{||}$ = 191.63 G and $g_{||}$ = 2.25 strongly support such coordination mode.[29,30,33] Moreover, similar EPR parameters are observed till pH 7.00 (Tab. 2), suggesting similar binding mode. Deprotonation of the last His (formation of CuL, maximum at pH 6.5) do not causes a large effect in UV-Vis and almost no effect in CD spectra which are more sensitive to complex geometry, from which we can conclusion that it does not participate in the binding; the CuL species is probably still a four-imidazole complex. In $CuH_{-1}L$ the coordination mode changes, what is clearly visible in all engaged techniques. Absorption band at 590 nm shifts to the lower wavelengths (blue-shift) to 540 nm what suggest amide nitrogen involvement in metal ion binding.[30] Looking at the EPR spectra, we observe change in the shape of spectra (Fig. 9) and, what is more convincing, change in spectroscopic (Tab. 2) and EPR parameters; stating from pH 8.00, $g_{||}$ is around or below 2.20, what is typical for 4N complexes as well, but with slightly different metal binding donor sets. Changes in the $g_{||}$ parameter could be derived from the involvement of the amide nitrogen in the metal binding $\{N^-, 3N_{im}\}$. The changes observed in the CD, UV-Vis spectra (Fig. 8) support the finding that the amide nitrogen displaces one of the histidine's imidazole. Above pH 8.5, the last 2 stable species are formed, $CuH_{-2}L$ and $CuH_{-3}L$. In this case, the metal ion coordination sphere includes the imidazole and three deprotonated amide nitrogens. The formation of the $CuH_{-3}L$ species results in the presence of a significant blue shift of the absorption band to 500 nm (Fig. 8A) together with the strong negative and positive band in CD spectra at 480 nm and 625 nm respectively (Fig. 8B).

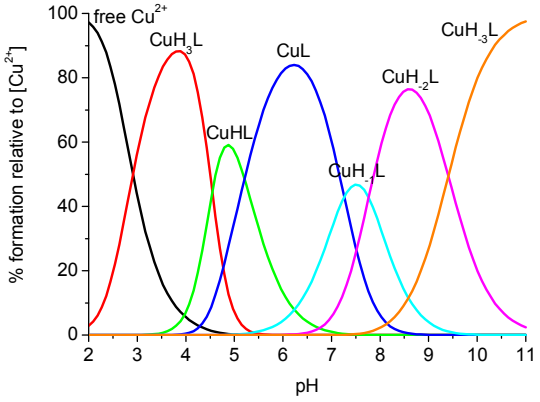

Fig. 7. Species distribution profiles for Cu^{2+} complexes of Ac-RAHAAHHRHSH-NH_2 peptide. Metal to ligand ratio = 1:1; [metal] = 1 x 10^{-3} M.

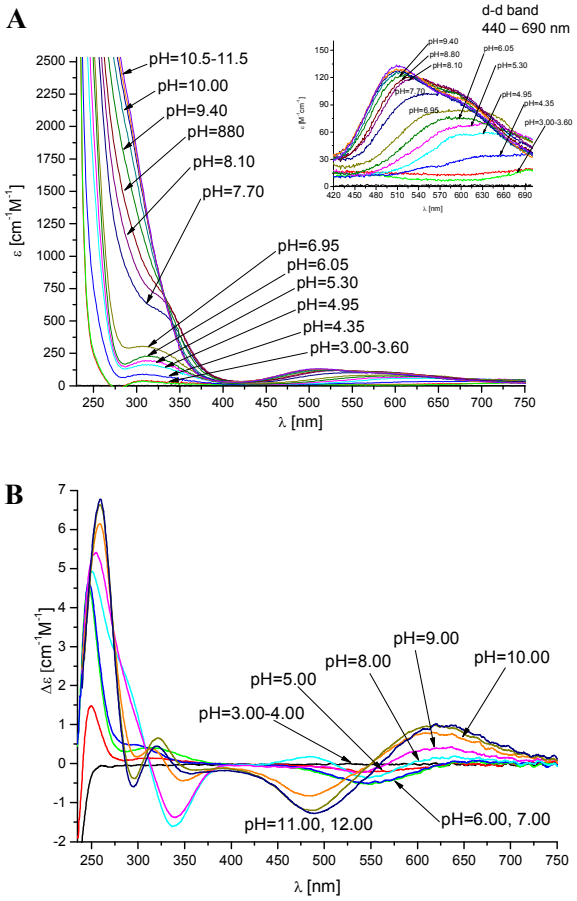

Fig. 8. UV-Vis (A) and CD spectra (B) for Cu^{2+} complex of Ac-RAHAAHHRHSH-NH_2 peptide. Metal to ligand ratio = 1:1; [metal] = 1 x 10^{-3} M.

Tab. 2. EPR data for pH-dependent Cu^{2+} complexes of Ac-RAHAAHHRHSH-NH_2 peptide.

pH	A_{II}	g_{II}
5.00	191.63	2.250
6.00	190.86	2.246
7.00	189.67	2.251
8.00	194.56	2.200
9.00	196.61	2.195
10.0	201.46	2.188
11.0	195.70	2.185
12.0	195.64	2.189

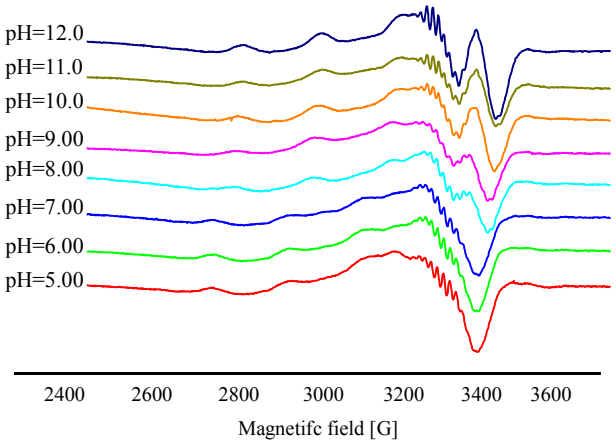

Fig. 9. EPR spectra performed for HRD-Cu^{2+} complexes, 5.00 – 12.00 pH range.

NMR of Cu^{2+} complexes is somewhat tricky because its unpaired electron influences the nuclear spin of the surrounding nuclei as well as longitudinal (R_1) and transverse (R_2) relaxation times giving rise to the paramagnetic effects.[36,37] Cu^{2+} ions have the ability to deprotonate and bind amide nitrogens when anchored to His imidazoles.[38] The broadening of side-chain protons, like for example those in imidazoles of His (Hδ, Hε) or γ nuclei of Glu, are mostly due to metal coordination to those residues; the same effects observed on backbone nuclei might prove binding to the main chain NH. Upon Cu^{2+} addition to the HRD free ligand, aromatic protons are vanished out almost completely; additionally the broadening of of His and Arg residues cross-peaks in the aliphatic region of ^1H–^1H TOCSY spectrum is observed, what suggest His imidazols in binding, especially those at the C-terminus of a peptide (Fig. 10 and 11). In this case, up to 0.25 Cu^{2+} eqs. were added to the free sample solutions. ^1H-^1H TOCSY NMR spectra recorded at pH 5.0 (where finger-print region is still well observable) in absence and in presence of substoichiometry amount of Cu^{2+} show the disappearance of particular His correlations and of cross-peaks belonging to neighboring to them residues; from finger-print region HN correlations with Hα, Hβ of His-193, Ser-194, His-195 and Arg-192 suggest this side of peptide being preferable (Fig. 11). All of these NMR data strongly indicate that all His imidazoles are involved in metal binding. Unfortunately the complete loss of NMR signals, detected in presence of higher metal concentrations, prevented us from obtaining further insights on the features of both Cu^{2+} complexes.

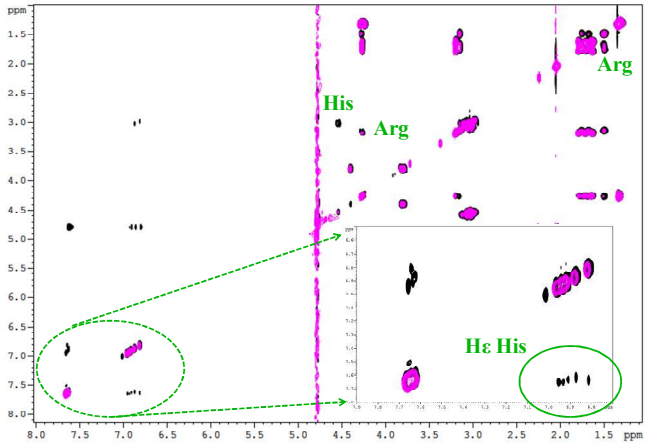

Fig. 10. ^1H-^1H TOCSY spectra of Ac-RAHAAHHRHSH-NH_2, 1 x 10^{-3} M, pH 7.0, T 300 K in absence (black) and in presence (magenta) of 0.25 Cu^{2+} eqs.

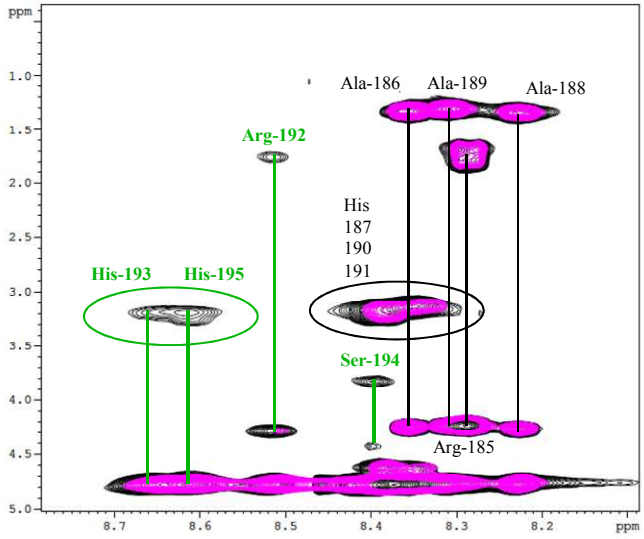

Fig. 11. Finger-print region of ^1H-^1H TOCSY spectra of Ac-RAHAAHHRHSH-NH_2, 1 x 10^{-3} M, pH 5.0, T 300 K, in absence (black) and in presence (magenta) of 0.10 Cu^{2+} eqs. The most affected correlations of HN with Hα, Hβ belonging to His, Arg and Ser residues are marked in green.

The very interesting part of this study appears when we try to compare the stability of Zn^{2+} and Ni^{2+} complexes. Looking at the potentiometric data, we may compare the logβ constant for ZnL and NiL complexes, 5.88 and 4.52 respectively, where only imidazoles are involved in binding. It seems quite clear, that Zn^{2+} complexes are more stable. Hypothetical simulation in the conditions where the amount of every reagent is equal (n_{Zn} : n_{Ni} : n_{HRD} = 1 : 1 : 1) shows Zn^{2+} species domination in whole pH range (Fig. 12). Taking into account described above NMR results we may withdraw a conclusion, that Zn^{2+} specificity for HRD studied fragment has a high impact on its complexes stability. This observation is very interesting, because Ni^{2+} complexes are usually more stable than Zn^{2+}.[39,40]

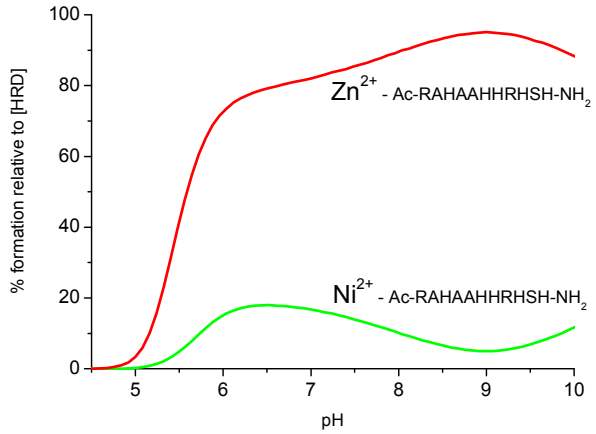

Fig. 12. Competition plot of Zn^{2+} and Ni^{2+} complexes with Ac-RAHAAHHRHSH-NH_2 (HRD); reagents molar ratio 1:1:1.

The behavior of HRD peptide is also interesting in the case of Cu^{2+} complexes. The competition plot with the peptide Ac-THHHHAHGG-NH_2 from Hpn protein (*Helicobacter pylori*)[41] revealed very high stability of a peptide from ZIP protein. In the case of HRD, the coordination of His imidazoles starts earlier (at more acidic pH) and the probability to form complexes with this peptide is incomparably higher than with Hpn. At pH slightly acidic, around 6.5, more than 80% of Cu^{2+} would be bound to the HRD (Fig. 13).

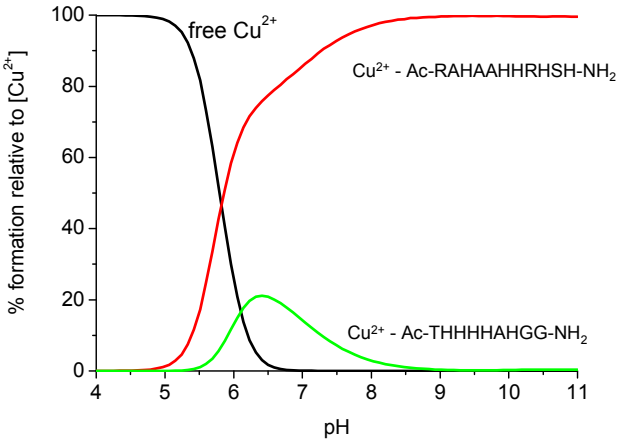

Fig. 13. A competition plot of the Ac-RAHAAHHRHSH-NH2 (HRD) and Ac-THHHHAHGG-NH_2 (Hpn) peptides with Cu^{2+} (1:1:1 molar ratio).

Experimental

Materials

The C- and N-protected peptide Ac-RAHAAHHRHSH-NH_2 was purchased from Selleck Chemicals (certified purity: 96.55%). Its purity was checked by using mass spectrometry. Moreover, the purity was evaluated based on potentiometric titrations using Gran method.[42] The solutions of metal ions were prepared using $CuCl_2$ x $2H_2O$, $NiCl_2$ x $6H_2O$ (Sigma Aldrich) and $ZnCl_2$ (POCh). The various metal salts were dissolved in filtered and double distilled water. The concentration of a stock solutions of these salts was measured by ICP-MS at least eight times and averaged for each of the metals. For the preparation of solutions of peptide was used 4 x 10^{-3} M HCl acid with the ionic strength 0.1 M (KCl, Sigma-Aldrich).

Potentiometry

Potentiometric measurements were performed at a constant temperature of 25°C under an argon atmosphere using a MOLSPIN pH-meter, equipped with a semi-combined electrode METTLER TOLEDO InLab® Micro and micrometer syringe with a volume of 0.23 cm^3. The measurements were performed in a pH range of 1.5 – 11.5. Before each measurement, the electrode was calibrated by titration of HCl (4 x 10^{-3} M) with a strong base NaOH (concentration 0.1025 M). The ligand and complexes pH-metric titrations were performed in water solution of HCl in 0.1 M KCl ionic strength. The titrant was carbonate-free (a standard solution of NaOH, 0.1025 M). The ligand concentration was 1 x 10^{-3} M and the metal to ligand molar ratios were 1 : 1. Stability constants for the proton, Zn^{2+}, Ni^{2+} and Cu^{2+} complexes were calculated from three titrations measured using a total volume of 1.5 cm^3. The data obtained in potentiometric measurements were analyzed using the HYPERQUAD 2006 program. Protonation constants of the ligands and overall stability constants (log βpqr) of the Cu^{2+}, Ni^{2+} and Zn^{2+} complexes were calculated by using equations (1) and (2).[43,44]

$$aM + bH + cL = M_aH_bL_c \quad (1)$$

$$\beta_{abc} = \frac{[M_aH_bL_c]}{[M]^a[H]^b[L]^c} \quad (2)$$

Standard deviations refer to random errors only. The speciation and competition diagrams were computed using the HySS 2006.

UV–Vis, CD and EPR spectroscopy

Measurements of the absorption UV-Vis spectroscopy was performed using a Cary 300 Bio spectrophotometer. CD spectroscopy of studied systems was performed on spectropolarimeter Jasco J-715 in a quartz cuvette path length of 0.1 and 1.0 cm, at 25°C using a total volume of 2.0 - 3.0 cm^3. UV-Vis and CD spectra of the Cu^{2+} and Ni^{2+} complexes were recorded in the same concentration and ligand : metal molar ratios as used for pH-potentiometry. The EPR continuous wave spectra were recorded in liquid nitrogen on a Bruker ELEXSYS E500 CW-EPR spectrometer at X-band frequency (9.5 GHz) and equipped with a cryostat of Oxford Instruments. The concentration of Cu^{2+} and peptides were the same as used for pH-potentiometry. The EPR parameters were calculated for the spectra obtained at the maximum concentration of the particular species for which well resolved separations were observed. Data were processed using the Origin 7.0.

Mass spectrometry

High-resolution mass spectra were obtained using a BrukerQ-FTMS spectrometer (Bruker Daltonik, Bremen, Germany), equipped with an Apollo II electrospray ionization source. Spectrometer was used in the range of positive values of m/z (mass to charge ratio) from 100 to 1500. The instrumental parameters were as follows: scan range m/z 400–2000, dry gas–nitrogen, temperature 170 °C, ion energy 5 eV, transfer time 120 ps. Capillary voltage was optimized and amounted 4500 V.

The small changes of voltage (±500 V) did not significantly affect the optimized spectra. The complexes were prepared in a 1:1 stoichiometry, [ligand] = 5 x 10^{-4} M was prepared in 1:1 MeOH-H_2O mixture. The instrument was calibrated by a TunemixTM solution. Data were processed by using the Bruker Compass DataAnalysis 4.0 program.

NMR

NMR experiments were carried out at 14.1 T at controlled temperature (±0.1 K) on a Bruker Advance III 600 MHz equipped with BBI probe, 5 mm, 1H/2H/31P-109Ag, Z-grad, ATMA. All samples were prepared in 10% D2O water solution (adjusting pH with NaOD and DCl). Suppression of water signal was achieved either by pre-saturation or by excitation sculpting [38] using a selective square pulse on water 2 ms long. Proton resonance assignment was obtained by ^{1}H-^{1}H 2D TOCSY, NOESY and ROESY experiments. Spectral processing was performed using the TopSpin v. 2.1.

Conclusions

The studied complexes of HRD peptide revealed very interesting chemical properties. The stability of its metal complexes increase in the series $Ni^{2+} < Zn^{2+} << Cu^{2+}$. Zn^{2+} ions bind to the peptide to three well defined His residues (Fig. 14). The addition of up to 1 equivalent of metal, causes the NMR shift of 3 His, which are in the middle of the peptide sequence.

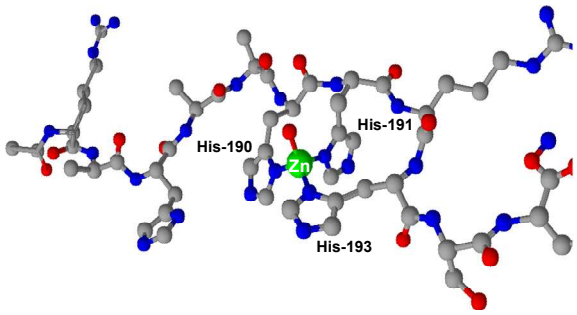

Fig. 14. Scheme of HRD-Zn^{2+} complex at pH 7.00. For clearer imaging, the hydrogens were removed; colors: silver, carbon; blue, nitrogen; red, oxygen; green, zinc. Figure was prepared in ACDLABS 12.0 (ChemSketch 3D).

Ni^{2+} complexes are the weakest. From the NMR measurements it is clear, that Ni^{2+} ions have more than one binding site in this short fragment. At pH 10, where complexes starts to be diamagnetic, shifts observed on the proton correlation spectra clearly evidence this physicochemical phenomenon. Ser-194 and Arg-192 suggest that preferable His residues are those at the C-terminus of the peptide; on the other hand, Ala residues shifts suggest other equally acceptable binding site. Comparison of Zn^{2+} and Ni^{2+} complexes revealed higher stability of Zn^{2+} complexes.

The answer to the question which His residues are preferable and thus most affected by Cu^{2+} ions is provided mostly in, so-called, finger-print region, where we may observe correlations of separated spin systems. Each amino acid, and thus correlations of HN with the protons from the side chain, lie in the same vertical line and can be distinguished easily. The broadening of the correlations belonging to Arg-192, Ser-194 and His-193 and 195 suggests C-terminus being preferential binding site. It is worth to mention, that in the case of nickel, also this side was observable; the behavior of those two metal ions is sometimes similar.[31]

No Cu^{2+} replacement with Zn^{2+} or even mixed complexes are formed; neither Zn^{2+} nor Ni^{2+} can substitute Cu^{2+} in the mixed metal complexes of HRD. They cannot even alter the distribution of Cu^{2+} ions among the various binding sites (no CD spectra change over titration of HRD-Cu^{2+} complex with Zn^{2+} and Ni^{2+} ions, data not shown). The reason is over 7 orders of magnitude difference comparing logβ of ZnL and CuL, but also the peptide length and limited number of binding sites located in close proximity; however, mixed Zn^{2+}, Ni^{2+} and Cu^{2+} complexes were sometimes observed.[45,46]

ZIP proteins are designed mainly to transport Zn^{2+} and/or Fe^{2+}, but several members are also selective for Mn^{2+}, Cu^{2+}, Ni^{2+} or Co^{2+}.[47-49] We believe that our study may give an additional clue to the understanding of the role of metal ions binding in crucial multi-histidine proteins.

Acknowledgements

The project is co-financed by the European Union as part of the European Social Fund.

Notes and references

[a] Faculty of Chemistry, University of Wroclaw, ul. Joliot-Curie 14, 50-383 Wroclaw, Poland.

[b] Department of Biotechnology, Chemistry and Pharmacy, via Aldo Moro 2, 53100 Siena, Italy.

† Electronic Supplementary Information (ESI) available: See DOI: 10.1039/b000000x/.

1 D. J. Eide. *Biochim. Biophys. Acta*, 2006, **1763**, 711.
2 U. Kra¨mer,, I. N. Talke, M. Hanikenne, *FEBS Lett.,* 2007, **581**, 2263.
3 X. Yang, J. Huang, Y. Jiang, H. S. Zhang,. *Mol. Biol. Rep.,* 2007, **24**, 1.
4 T. Mizuno, K. Hirano, S. Kato, H. Obata, Soil Sci. *Plant Nutr.*, 2008, **54**, 86.
5 G. Schmitt-Ulms, S. Ehsani, J. C. Watts, D. Westaway, H. Wille. *PLoS One*, 2009, **28**, 4(9), e7208.
6 S. Ehsani, R. Tao,C. L. Pocanschi, H. Ren, P. M. Harrison, G. Schmitt-Ulms. *PLoS ONE*, 2011, **6**, 10, e26800.
7 S. Potocki, M. Rowinska-Zyrek, D. Valensin, K. Krzywoszynska, D. Witkowska, M. Luczkowski, H. Kozlowski, *Inorg. Chem.,* 2011, **50**, 6135.
8 E. E. Rogers, D. J. Eide, M. Lou Guerinot, *PNAS*, 2000, **97**, 22, 12356.
9 S. Potocki, D. Valensin, F. Camponeschi, H. Kozlowski, *J. Inorg. Biochem.,* 2013, **127**, 246.
10 S. Nishida, Y. Morinaga, H. Obata, T. Mizuno. *FEBS J.,* 2011, **278**, 851.
11 B. Milon, Q. Wu, J. Zou, L. C. Costello, R. B. Franklin. *Biochim. Biophys. Acta*., 2006, **1758**, 1696.
12 R. S. Gitan, M. Shababi, M. Kramer, D. J. Eide. *J. Biol. Chem.,* 2003, **278**, 39558.
13 M. Takafumi, U. Koji, N. Syo, U. Takanori, O. Hitoshi, *Plant Phys. Biochem.*, 2007, **45**, 371.

14 S. Nishida, T. Mizuno, H. Obata. *Plant Phys. Biochem.,* 2008, **46**, 601.

15 X. Mao, B. E. Kim, F. Wang, D. J. Eide, M. J. Petris, *J. Biol. Chem.*, 2007, **282**, 6992.

16 C. Murgia, I. Vespignani, J. Cerase, F. Nobili, G. Perozzi, *Am. J. Physiol.* 1999, **277**, 1231.

17 M. W. Persans, K. Nieman, D. E. Salt, *Proc. Natl. Acad. Sci. USA*, 2001, **98**, 9995.

18 E. L. Connolly, J. P. Fett, M. Lou Guerinot, *Plant Cell*, 2002, **14**, 1347.

19 T. Mizuno, K. Usui, K. Horie, S. Nosaka, N. Mizuno, H. Obata. *Plant Physiol. Biochem.*, 2005, **43**, 793.

20 M. Takafumi, U. Koji, N. Syo, U. Takanori, O. Hitoshi, *Plant Phys. Biochem.*, 2007, **45**, 371.

21 C. Kállay, K. Ősz, A. Dávid, Z. Valastyán, G. Malandrinos, N. Hadjiliadis, I. Sóvágó. *Dalton Trans.*, 2007, 4040.

22 C. Migliorini, D. Witkowska, D. Valensin, W. Kamysz, H. Kozlowski, *Dalton Trans.*, 2010, **39**, 8663.

23 M. A. Zoroddu, M. Peana, S. Medici, S. Potocki, H. Kozlowski, *Dalton Trans.*, 2014, **43**, 2764.

24 R. A. Ingle, S. T. Mugford, J. D. Rees, M. M. Campbell, J. A. C. Smith, *Plant Cell*, 2005, **17**, 2089.

25 D. Valensin, M. Luczkowski, F.M. Mancini, A. Legowska, E. Gaggelli, G. Valensin, K. Rolka, H. Kozłowski, *Dalton Trans.*, 2004, 1284.

26 P. Stańczak, M. Luczkowski, P. Juszczyk, Z. Grzonka, H. Kozłowski, *Dalton Trans.*, 2004, 2007.

27 C. Migliorini, D. Witkowska, D. Valensin, W. Kamysz, H. Kozlowski, *Dalton Trans.*, 2010, **39**, 8663.

28 A. Sigel (Editor), H. Sigel (Editor), R. K. O. Sigel (Editor), *Nickel and Its Surprising Impact in Nature: Metal Ions in Life Sciences*, Vol. 2, ISBN: 978-0-470-01671-8728 pages, February 2007.

29 M. Rowinska-Zyrek, D. Witkowska, D. Valensin, W. Kamysz and H. Kozłowski, *Dalton Trans.,* 2010, **39**, 5814.

30 K. Kulon, D. Wozniak, K. Wegner, Z. Grzonka and H. Kozlowski, *J. Inorg. Biochem.*, 2001, **101**, 1699.

31. L. D. Pettit, J. E. Gregor, H. Kozlowski. *Perspect. Bioinorg. Chem.*, Vol. 1, R. W. Hay, J. R. Dilworth, K. B. Nolan, JAI Press, London, p.1, 1991.

32 T. Kowalik-Jankowska, H. Kozlowski, E. Farkas, I. Sovago, *Metal Ions in Life Sciences*, 2, 63-108, eds. Sigel A., Sigel H., Sigel R. K. O., John Wiley & Sons, Ltd., 2007.

33 D. Witkowska, D. Valensin, M. Rowinska-Zyrek, A. Karafova, W. Kamysz, H. Kozlowski, *J. Inorg. Biochem.*, 2012, **107**, 73.

34 E. Gaggelli, H. Kozlowski, D. Valensin, G. Valensin, *Chem. Rev.,* 2006, **106**, 1995.

35 H. Kozlowski, W. Bal, M. Dyba, T. Kowalik-Jankowska, *Coord. Chem. Rev.* 1999, **184**, 319.

36 L. Banci, I. Bertini and C. Luchinat, *Nuclear and Electron Relaxation: The Magnetic Nucleus-Unpaired Electron Coupling in Solution*, Wiley-VCH, Weinheim, 1991.

37 I. Bertini, C. Luchinat, G. Parigi, *Solution NMR of Paramagnetic Molecules: Applications to Metallobiomolecules and Models*; Volume 2, Elsevier Science, Amsterdam, 2011.

38 H. Kozłowski, T. Kowalik-Jankowska, M. Jeżowska-Bojczuk, *Coord. Chem. Rev.* 2005, **249**, 2323.

39 M. Rowinska-Zyrek, S. Potocki, D. Witkowska, D. Valensin, H. Kozlowski, *Dalton Trans.*, 2013, **42**, 6012.

40 M. Rowinska-Zyrek, S. Potocki, D. Witkowska, D. Valensin, H. Kozlowski, *Dalton Trans.*, 2013, **42**, 6012.

41 D. Witkowska, R. Politano, M. Rowinska-Zyrek, R. Guerrini, M. Remelli, H. Kozlowski, *Chem. Eur. J.*, 2012, **18**, 11088.

42 G. Gran, *Acta Chem. Scand.*, 1950, **4**, 559.

43 P. Gans, A. Sabatini, A. Vacca, *Dalton Trans.*, 1985, 1195.

44 T. L. Hwang, A. J. Shaka, *J. Magn. Reson.*, 1995, **112**, 275.

45 V. Jószai, I. Turi, C. Kállay, G. Pappalardo, G. Di Natale, E. Rizzarelli, I. Sóvágó, *J. Inorg. Biochem.*, 2012, **112**, 17.

46 E. Józsa, K. Osz, C. Kállay, P. de Bona, C. A. Damante, G. Pappalardo, E. Rizzarelli, I. Sóvágó, *Dalton Trans.,* 2010, **14**, 7046.

47 R. Shingles, L. E. Wimmers, R. E. McCarty, *Plant Physiol.*, 2004, **135**, 145.

48 G. Grass, S. Franke, N. Taudte, D. H. Nies, L. M. Kucharski, M. E. Maguire, C. Rensing, *J. Bacteriol.*, 2005, **187**, 1604.

49 S. Nishida, C. Tsuzuki, A. Kato, A. Aisu, J. Yoshida, T. Mizuno, *Plant Cell Physiol.* 2011, **52**, 1433.